Supporting Information

Ambient Size Distributions and Lung Deposition of Aerosol Dithiothreitol-Measured Oxidative Potential: A Contrast Between Soluble and Insoluble Particles

Ting Fang[a], Linghan Zeng[a], Dong Gao[b], Vishal Verma[c], Aleksandr B. Stefaniak[d], Rodney J. Weber[a]*

[a] School of Earth and Atmospheric Sciences, Georgia Institute of Technology, Atlanta, GA, 30332, USA

[b] School of Civil and Environmental Engineering, Georgia Institute of Technology, Atlanta, GA, 30332, USA

[c] Department of Civil and Environmental Engineering, University of Illinois Urbana-Champaign, Champaign, IL, 61801, USA

[d] Respiratory Health Division, National Institute for Occupational Safety and Health, Morgantown, WV, 26505, USA

*Corresponding author
Professor Rodney J. Weber, Ph.D.
Georgia Institute of Technology
School of Earth and Atmospheric Sciences
311 Ferst Drive Atlanta GA, 30332
office phone: 404.894.1750
Email: rodney.weber@eas.gatech.edu

Number of page	12
Number of figures	10
Number of tables	7

Detailed method to account for the non-uniform deposits of particles on MOUDI filters:

The MOUDI sampler collects particles as discrete points on the substrate filter, each point being associated with an impact jet. For the upper size stages where the number of impactor jets are few, this leads to highly non-uniform deposits. This raises issues when cutting the filter and for the OCEC analysis, which depends on a laser transmission through the filter to assess the split in OC and EC. At smaller size stages the number of jets is so large that the deposit can be assumed to be uniform. In order to calculate the total deposits of different chemical components on the filters, the chemical mass on the corresponding filter portion was multiplied by the ratio of the number of dots on the whole filter versus those on the analyzed filter portion. This was done for stages with a cut size larger than 0.56 μm; for smaller stages with 900 to 2000 nozzles, ratios of filter surface areas were used.

Since the laser beam in the OCEC analyzer may pass through blank filter space due to the non-uniform deposition in MOUDI samples, OC/EC separation was done using a manual split at 800 seconds. This specific split time was based on the split time (800 ± 100 s) obtained from a set of uniform deposited filter samples collected at another urban site in Atlanta, GA. Split times of 700 and 900 seconds were applied to the data and shown as error bars on OC and EC distributions in Figure S8&9.

Table S1. Summary of MOUDIs filter collection and analysis

Season Year	Sampling Period	RS (road-side)		GT (urban)	
		MOUDI #1	**MOUDI #2**	**MOUDI #1**	**MOUDI #2**
Summer 2015	7/6-7/13/2015			*Teflon (OP_{ws}^{DTT})	
	7/23-7/30/2015		Teflon (OP_{ws}^{DTT})	Teflon (OP_{ws}^{DTT})	
	8/3-8/11/2015	Teflon (OP_{ws}^{DTT})			
Fall 2015	9/16-9/24/2015			Teflon (OP_{ws}^{DTT})	Quartz (OC, EC, ions)
	10/6-10/14/2015	Teflon (OP_{ws}^{DTT})	Quartz (OC, EC, ions)		
Spring 2016	3/16-3/23/2016			Teflon (OP_{ws}^{DTT}, OP_{total}^{DTT})	Quartz (OC, EC, ions, metals)
	3/28-4/4/2016	Teflon (OP_{ws}^{DTT}, OP_{total}^{DTT})	Quartz (OC, EC, ions, metals)		
	4/18-4/25/2016		Teflon (OP_{ws}^{DTT}, OP_{total}^{DTT})	Teflon (OP_{ws}^{DTT}, OP_{total}^{DTT})	

* filter type (species measured), Organic carbon (OC), elemental carbon (EC), ions, and metals were determined from the pre-baked quartz filters (47 mm, Tissuquartz™ Filters, Pall Corp., Ann Arbor, MI, USA), and the Zefluor filters (47 mm PTFE Membrane Filters, 2 μm pore size, Pall Corp., Ann Arbor, MI, USA) were used for determining the OP of particles.; OP_{ws}^{DTT} – water-soluble DTT activity; OP_{total}^{DTT} – total DTT activity.

Equations to fit the distributions:

$$\frac{dC}{dlnD_p} = \frac{C_t}{(2\pi)^{1/2} ln\sigma_g} \exp\left(-\frac{(lnD_p - lnGMD)^2}{2ln^2\sigma_g}\right),$$

where C is the concentration of PM species (μg m^{-3} or ng m^{-3}) or oxidative potential per volume of air (OP, nmol min^{-1} m^{-3}), D_p is the aerodynamic diameter (μm), and GMD and σ_g are geometric mean diameter (μm) and geometric standard deviation for the lognormal fits. C_t is the total level of PM species or OP; it's the area under the curve, same unit as C.

Averaged frequency OP distribution:

$$\frac{df}{dlnD_p} = \frac{1}{(2\pi)^{1/2} ln\sigma_{g_{mean}}} \exp\left(-\frac{(lnD_p - lnGMD_{mean})^2}{2ln^2\sigma_{g_{mean}}}\right),$$

where GMD_{mean} and $\sigma_{g_{mean}}$ are the mean of the GMD and σ_g obtained from a lognormal fit of each MOUDI sets, respectively.

Table S2. Summary of size distribution geometric mean diameters (GMD) in μm for lognormal fits of OP from all MOUDIs sets collected in Atlanta, GA (Parameters for OP_{wi}^{DTT} are shown for fine and coarse mode due to bimodal distribution)

Season Year	Sampling Period	RS (road-side)			GT (urban)		
		OP_{ws}^{DTT}	OP_{wi}^{DTT}		OP_{ws}^{DTT}	OP_{wi}^{DTT}	
			Fine	coarse		Fine	coarse
Summer 2015	7/6-7/13/2015	-	-	-	1.00	-	-
	7/23-7/30/2015	0.87	-	-	0.94	-	-
	8/3-8/11/2015	1.03	-	-	-	-	-
Fall 2015	9/16-9/24/2015	-	-	-	1.10	-	-
	10/6-10/14/2015	2.51	-	-	-	-	-
Spring 2016	3/16-3/23/2016	-	-	-	0.80	0.35	4.76
	3/28-4/4/2016	1.77	0.12	3.76	-	-	-
	4/18-4/25/2016	1.13	0.32	3.48	0.87	0.46	5.50
* GMD, **Mean ± SD**		**1.46 ± 0.68**	**0.22 ± 0.14**	**3.62 ± 0.20**	**0.94 ± 0.12**	**0.41 ± 0.07**	**5.13 ± 0.52**

Table S3. Summary of size distribution geometric standard deviation (σ_g) [unitless] for lognormal fits of OP from all MOUDIs sets collected in Atlanta, GA (Parameters for OP_{wi}^{DTT} are shown for fine and coarse mode due to bimodal distribution)

Season Year	Sampling Period	RS (road-side)			GT (urban)		
		OP_{ws}^{DTT}	OP_{wi}^{DTT}		OP_{ws}^{DTT}	OP_{wi}^{DTT}	
			Fine	coarse		Fine	coarse
Summer 2015	7/6-7/13/2015	-	-	-	5.36	-	-
	7/23-7/30/2015	5.21	-	-	5.21	-	-
	8/3-8/11/2015	5.69	-	-	-	-	-
Fall 2015	9/16-9/24/2015	-	-	-	6.49	-	-
	10/6-10/14/2015	2.89	-	-	-	-	-
Spring 2016	3/16-3/23/2016	-	-	-	5.59	2.29	2.33
	3/28-4/4/2016	5.79	2.16	2.74	-	-	-
	4/18-4/25/2016	6.03	1.35	1.55	7.38	1.36	1.87
* σ_g, **Mean ± SD**		**5.12 ± 1.28**	**1.75 ± 0.57**	**2.14 ± 0.84**	**6.01 ± 0.92**	**1.83 ± 0.66**	**2.10 ± 0.32**

Table S4. Summary of total OP (OPt) for each lognormal fit of OP [nmol min^{-1} m^{-3}] from all MOUDIs sets collected in Atlanta, GA (Parameters for OP_{wi}^{DTT} are shown for fine and coarse mode due to bimodal distribution)

Season Year	Sampling Period	RS (road-side)			GT (urban)		
		OP_{ws}^{DTT}	OP_{wi}^{DTT}		OP_{ws}^{DTT}	OP_{wi}^{DTT}	
			Fine	coarse		Fine	coarse
Summer 2015	7/6-7/13/2015	-	-	-	0.18	-	-
	7/23-7/30/2015	0.21	-	-	0.20	-	-
	8/3-8/11/2015	0.25	-	-	-	-	-
Fall 2015	9/16-9/24/2015	-	-	-	0.21	-	-
	10/6-10/14/2015	0.27	-	-	-	-	-
Spring 2016	3/16-3/23/2016	-	-	-	0.16	0.10	0.07
	3/28-4/4/2016	0.20	0.04	0.07	-	-	-
	4/18-4/25/2016	0.27	0.02	0.27	0.22	0.02	0.03
* OPt, **Mean ± SD**		**0.24 ± 0.03**	**0.03 ± 0.01**	**0.17 ± 0.14**	**0.20 ± 0.02**	**0.06 ± 0.06**	**0.05 ± 0.03**

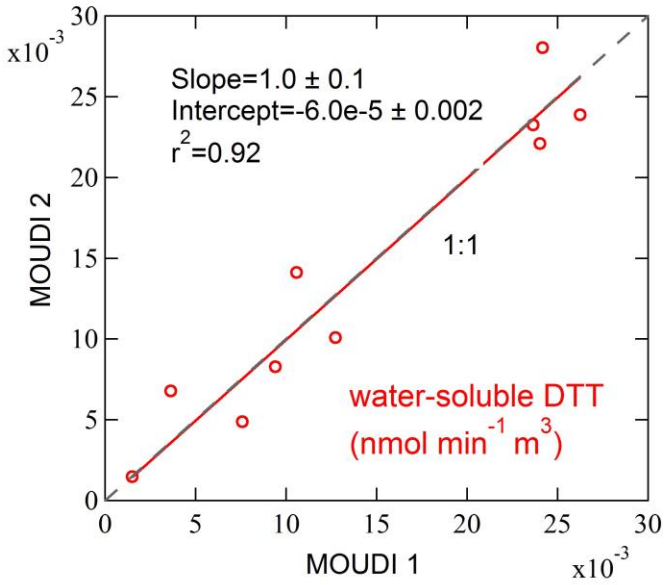

Figure S1. Comparison between two MOUDIs deployed side-by-side at the GT site where OP_{ws}^{DTT} were measured on each stage. Each data point is for the same impactor stage on the two MOUDIs. Linear fits were done by orthogonal regression. The dotted line is 1:1.

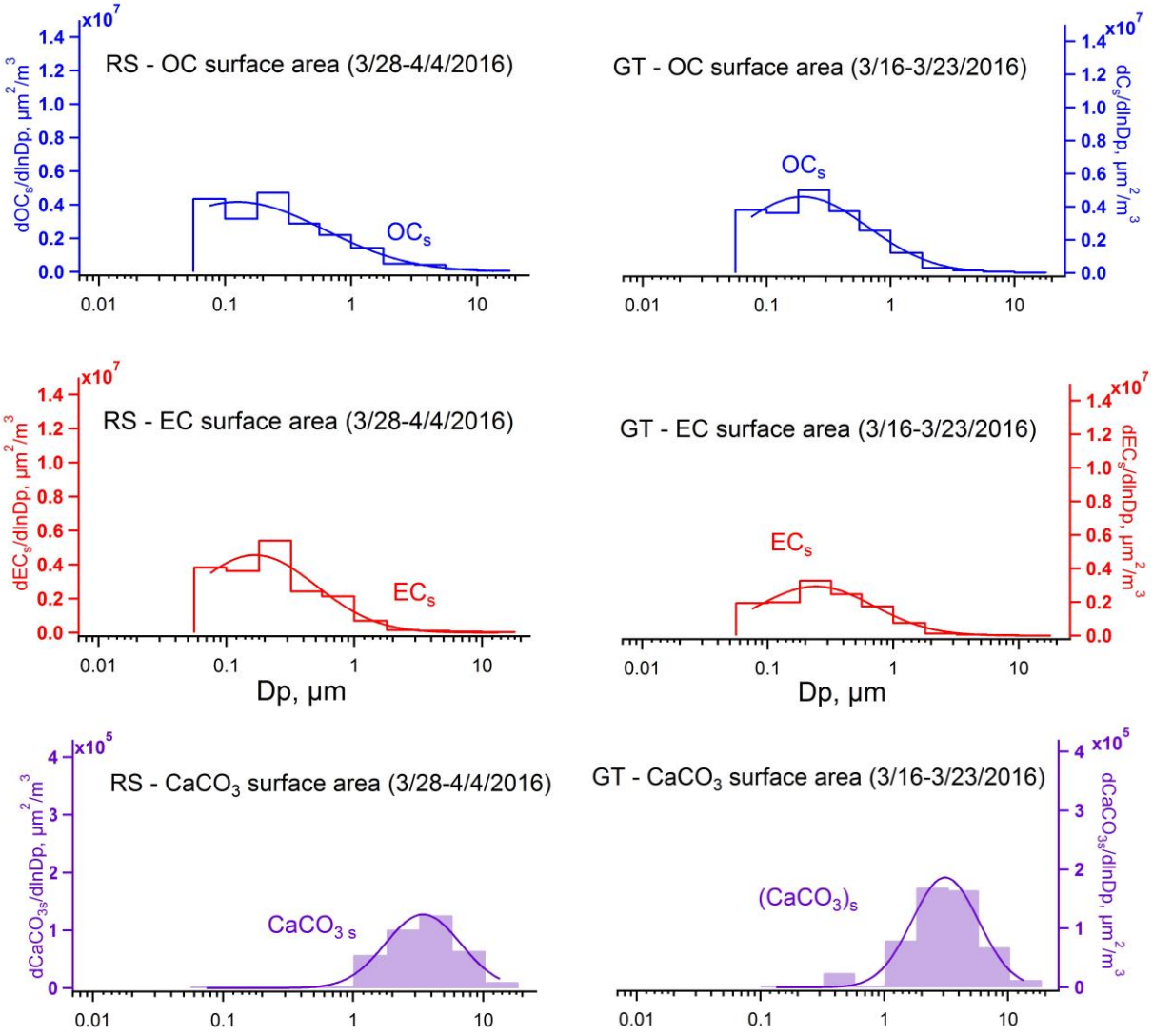

Figure S2. Surface area distribution of OC, EC, and $CaCO_3$ from MOUDI set collected in spring 2016.

Detailed method for measuring total DTT activity on MOUDIs filters:

a) **Filter extraction**: filter sample (half of a 47 mm MOUDI Teflon filter) was sonicated in 4.9 mL DI water in a 15 mL centrifuge tube for 30 min with an Ultrasonic Cleanser (VWR International LLC, West Chester, PA, USA);

b) **Total DTT activity (OP_{total}^{DTT}) measurement**:
After sonication, 1.4 mL potassium phosphate buffer (pH = 7.4) was added to the centrifuge tube containing the sample filter and extract, after that the tube was placed in a ThermoMixer (Eppendorf North America, Inc., Hauppauge, NY, USA) for approximately 5 min to ensure the temperature of the tube reached 37 °C. At time zero, 0.7 mL 1mM DTT solution was added to the Kbuffer-sample mixture. DTT was consumed over time. At five different time intervals (7, 15, 25, 32, 40 min), 100 µL of the mixture was transferred to another centrifuge tube preloaded with 1 mL 1% v/v Trichloroacetic acid (TCA) to quench the DTT consumption. To determine the concentration of DTT remaining in the tube, 2 mL Tris buffer (0.08 M with 4 mM EDTA) and 0.2 mL DTNB (0.5 mM) were added to the quenched mixture with residual DTT. Reaction between the residual DTT and DTNB forms a light absorbing compound, 2-nitro-5-thiobenzoic acid (TNB), which has a high extinction coefficient at 412 nm wavelength. The final mixture with TNB was then passed through a Liquid Waveguide Capillary Cell (LWCC-M-100; World Precision Instruments, Inc., FL, USA) coupled to a UV-VIS light source (Ocean Optics DT-Mini-2B, Ocean Optics, Inc., Dunedin, FL, USA), and a multi-wavelength light detector (USB4000 Miniature Fiber Optic Spectrometer, Ocean Optics, Inc., Dunedin, FL, USA) to determine the absorbance at 412 nm wavelength, respectively. The absorbance measured via this method was calibrated with known concentration of DTT, and the calibration curve was used to calculate the remaining amount of DTT in the sample-Kbuffer-DTT mixture.

c) **Final OP calculations**:

The final OP can be calculated as follows:

$$OP\ (nmol\ min^{-1}\ m^{-3}) = \frac{\sigma_{sample}(nmol\ min^{-1}) - \sigma_{blank}(nmol\ min^{-1})}{\frac{V_a\ (mL)}{V_e\ (mL)} \times V_p(m^3) \times \frac{A_p}{A_{total}}} \qquad \text{Eq. (1)}$$

σ_{sample} and σ_{blank} are the consumption rates of sample and blank, i.e. the slopes by taking a linear fit to the remaining amount of DTT in the sample-Kbuffer-DTT mixture over time (nmol min^{-1}); V_e and V_a are the extraction volume and sample volume added to the sample-Kbuffer-DTT mixture, respectively; V_p is the total air volume sampled through the whole filter; A_{total} and A_p are total area and the area taken for OP analysis,

respectively. For stages with a cut-off size of 0.56 µm and up, A_{total} and A_p represent the number of dots on the whole Teflon filter and that taken for OP analysis.

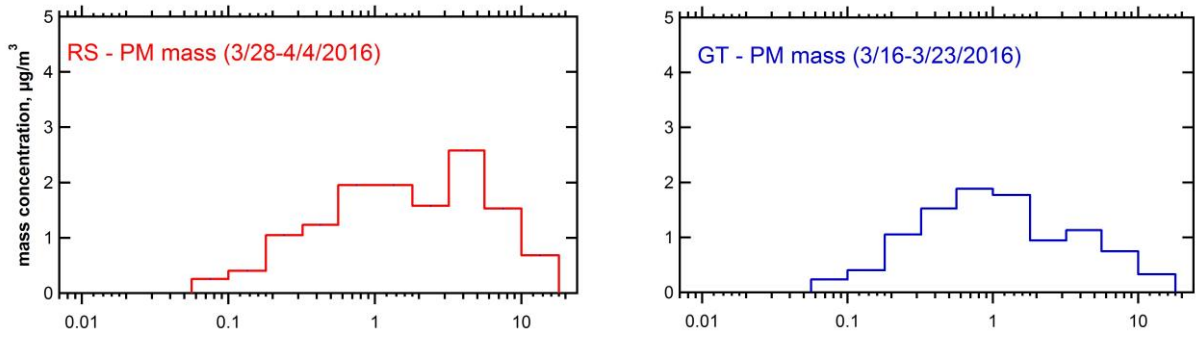

Figure S3. Estimated PM mass size distribution from the sum of elemental carbon (EC), organic mass (OC*1.6), total metals, and ions (SO_4^{2-}, NO_3^-, Cl^-, and NH_4^+) from MOUDI samples collected in Spring 2016. Total metals were represented by their oxides forms (K_2O, $CaCO_3$, MgO, CuO, MnO_2, and Fe_2O_3), except for Cu and Mn that their total metals (elemental) were used for stages below 1.8 µm, given that Cu and Mn particles smaller than 1.8 µm are mostly water-soluble [1] and metal sulfates [2, 3].

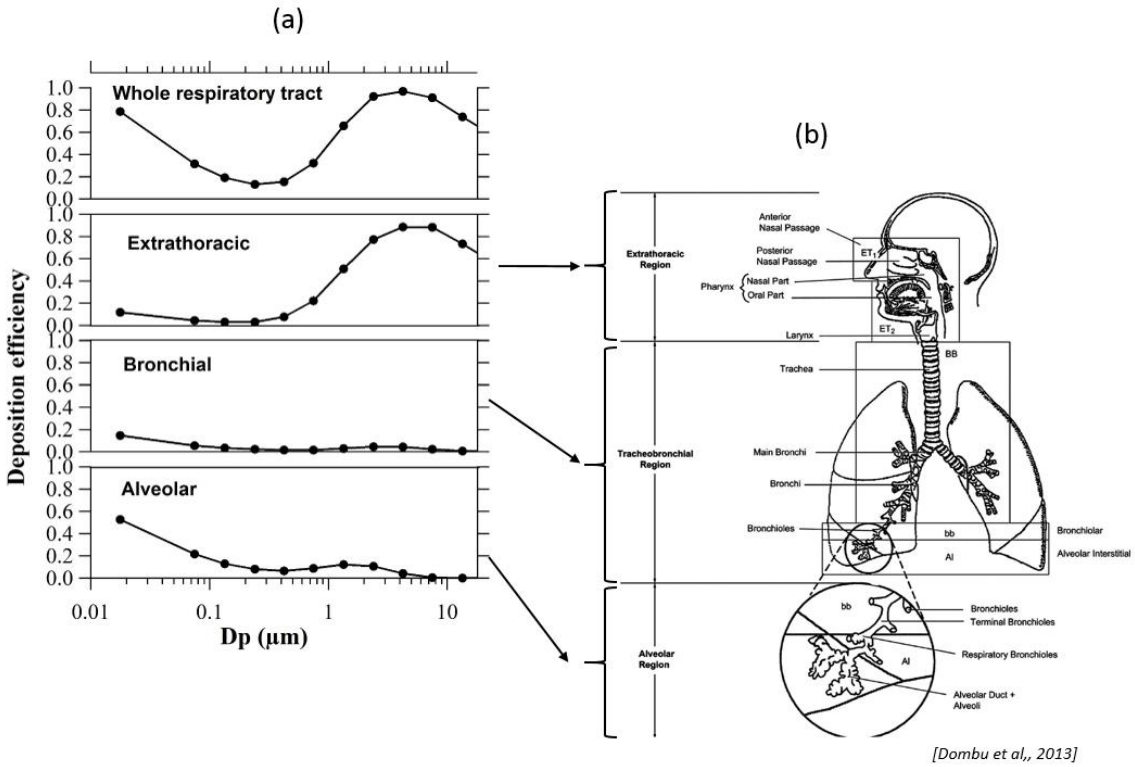

Figure S4. Whole respiratory tract and regional deposition efficiency of aerosols assuming unit density spherical particle and nose-only breathing at a steady breathing with a flow rate of 1.5 m^3 h^{-1}, respiration frequency of 20 min^{-1}, and tidal volume of 1250 cm^3. Regional deposition refers to the collection of particles in extrathoracic, bronchial, and alveolar regions. (b) was adapted from Dombu et al., 2013 [4].

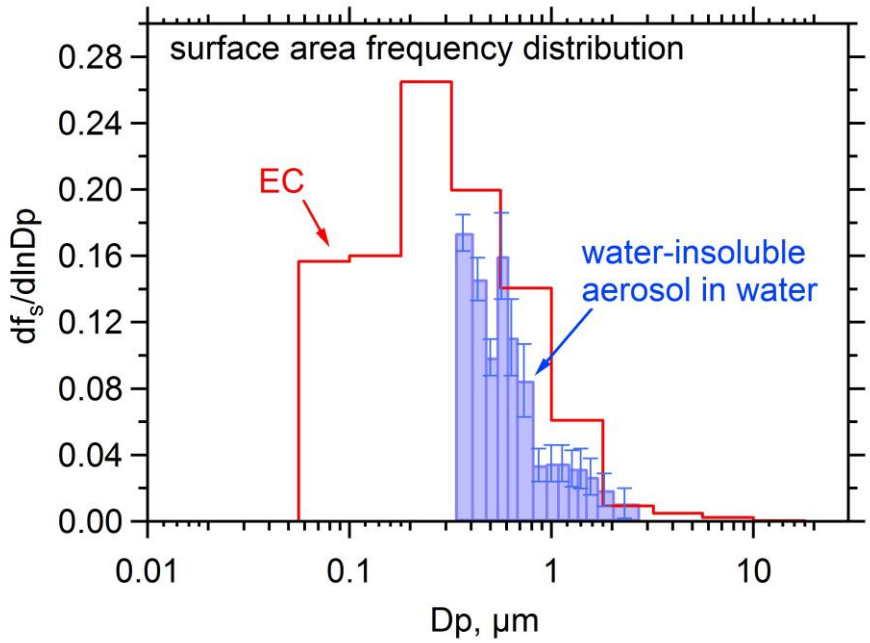

Figure S5. Water-insoluble aerosol (WIA) surface area frequency distribution adapted from the number concentration distribution from Greenwald et al. [5] in comparison with EC surface area frequency distribution at the urban site from this work. The WIA instrument collects ambient aerosols into water with a high flow rate liquid impinger and measures the solid particles in the liquid with optical diameters from 0.25 to 2.0 µm with an optical particle counter to determine the number concentration distribution of ambient insoluble particles in water. This WIA instrument provides evidence of the size distribution of insoluble particles when deposited in the lung, in contrast to the distribution in the ambient atmosphere that may be internally mixed with soluble species, assuming the water-soluble components have similar solubilities in water as lung lining fluid. The surface area function was calculated from the measured number concentration using the equation $\frac{dS}{d\ln D_p} = \frac{dN}{d\ln D_p} \pi D_{pg}^2$, where D_p and D_{pg} is the aerodynamic and geometric mean aerodynamic diameter in each MOUDI stage (µm). The optical diameter from Greenwald et al. [5] was converted to aerodynamic D_p using the equation $D_p = D_{optical}\ \rho^{0.5}$ (referred to Murphy et al. [6]), where $D_{optical}$ is the optical diameter (µm) and ρ is the density, 1.77 g cm^{-3}. Error bars on the WIA surface distribution represent the standard deviations from four sets of data collected from May to June in 2004.

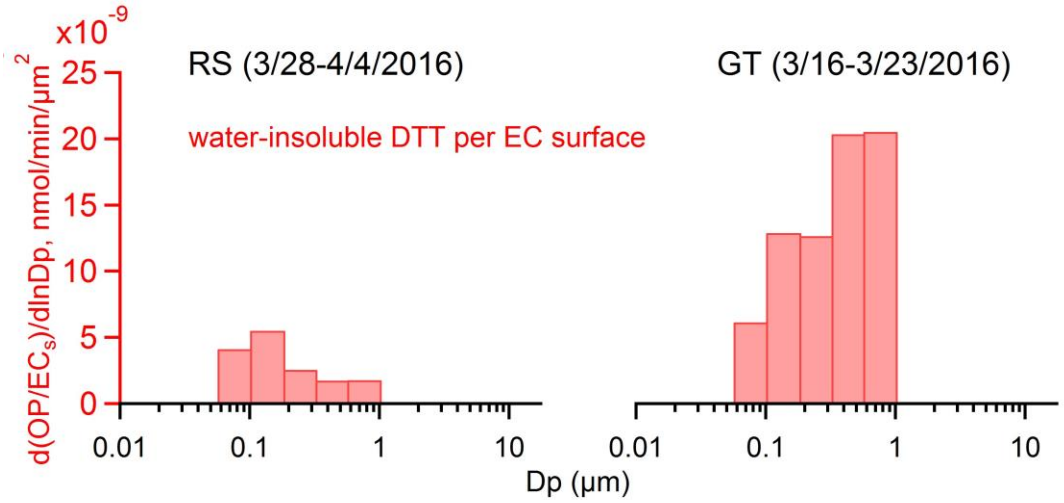

Figure S6. Water-insoluble DTT per EC surface area for Dp smaller than 1 µm. MOUDI samples were collected during different time periods at a road-side (RS) and urban (GT) site in Atlanta. OP_{wi}^{DTT} per EC surface area (mean ± standard deviation) was (1.5 ± 0.6) × 10^{-8} and (3.2 ± 1.6) × 10^{-9} nmol min^{-1} μm^{-2} for GT and RS, respectively,

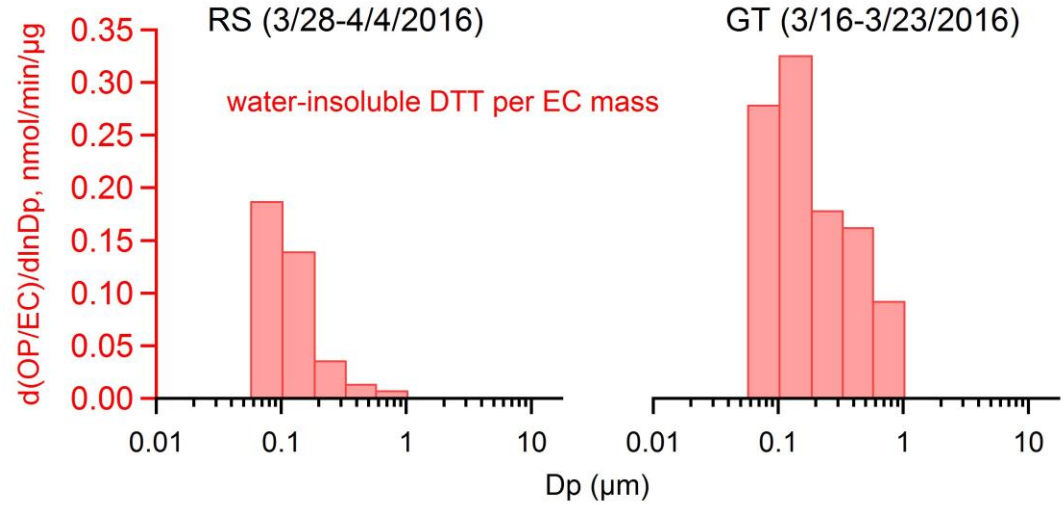

Figure S7. Water-insoluble DTT per EC mass for Dp smaller than 1 µm. MOUDI samples were collected during different time periods at a road-side (RS) and urban (GT) site in Atlanta. OP_{wi}^{DTT} per EC mass (mean ± standard deviation) was 0.21 ± 0.09 and 0.08 ± 0.08 nmol min^{-1} μg^{-1} for GT and RS, respectively.

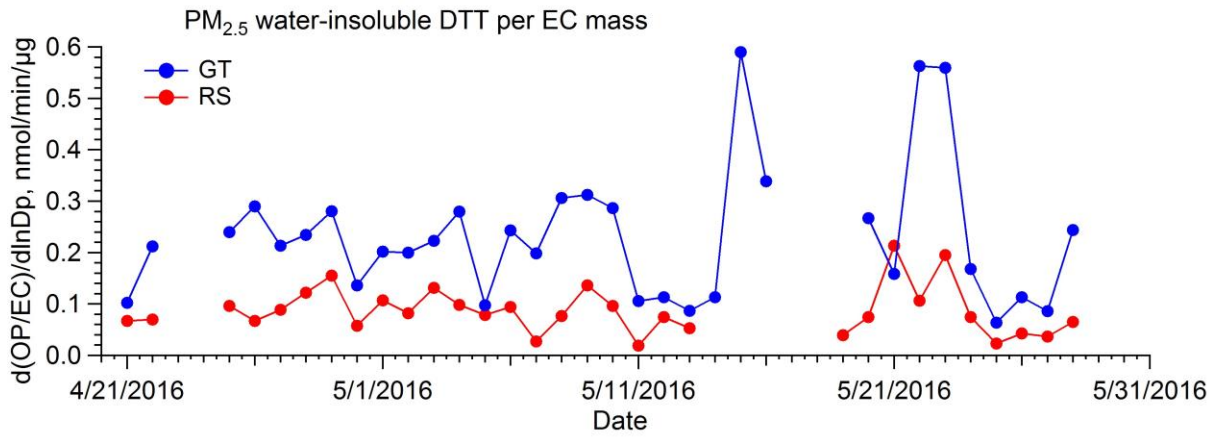

Figure S8. Water-insoluble DTT per EC mass from $PM_{2.5}$ samples collected on filters at road-side (RS) and urban site (GT). OP_{wi}^{DTT} per EC mass was 0.23 ± 0.13 and 0.09 ± 0.05 nmol min^{-1} μg^{-1} for GT and RS, respectively.

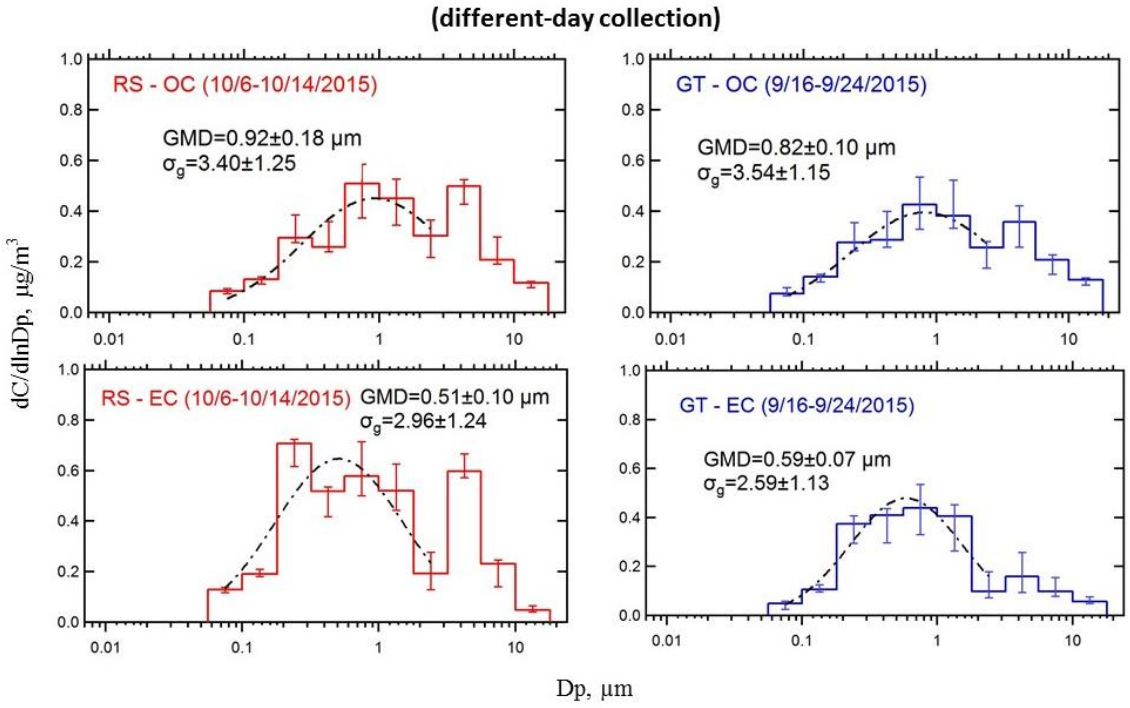

Figure S9. Ambient size distribution of OC and EC from MOUDI sets collected in fall 2015.

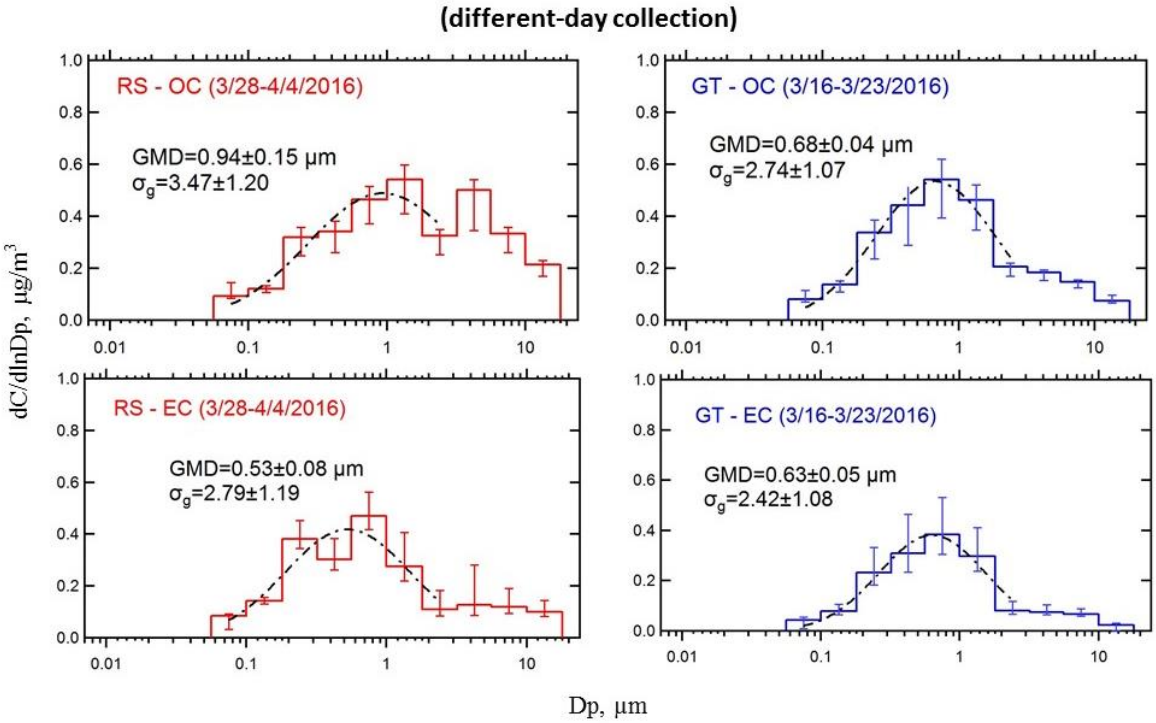

Figure S10. Ambient size distribution of OC and EC from MOUDI sets collected in spring 2016.

References

1. Fang, T.; Guo, H.; Zeng, L.; Verma, V.; Nenes, A.; Weber, R. J., Highly acidic ambient particles, soluble metals, and oxidative potential: a link between sulfate and aerosol toxicity. *Environ. Sci. Technol.* **2017**.
2. Oakes, M.; Ingall, E. D.; Lai, B.; Shafer, M. M.; Hays, M. D.; Liu, Z. G.; Russell, A. G.; Weber, R. J., Iron solubility related to particle sulfur content in source emission and ambient fine particles. *Environ. Sci. Technol.* **2012,** *46*, (12), 6637-6644.
3. Longo, A. F.; Vine, D. J.; King, L. E.; Oakes, M.; Weber, R. J.; Huey, L. G.; Russell, A. G.; Ingall, E. D., Composition and oxidation state of sulfur in atmospheric particulate matter. *Atmos. Chem. Phys.* **2016,** *16*, (21), 13389-13398.
4. Dombu, C. Y.; Betbeder, D., Airway delivery of peptides and proteins using nanoparticles. *Biomaterials* **2013,** *34*, (2), 516-25.
5. Greenwald, R.; Bergin, M. H.; Weber, R.; Sullivan, A., Size-resolved, real-time measurement of water-insoluble aerosols in metropolitan Atlanta during the summer of 2004. *Atmos. Environ.* **2007,** *41*, (3), 519-531.
6. Murphy, D. M.; Cziczo, D. J.; Hudson, P. K.; Schein, M. E.; Thomson, D. S., Particle density inferred from simultaneous optical and aerodynamic diameters sorted by composition. *J. Aerosol Sci.* **2004,** *35*, (1), 135-139.